Activation of protein kinase C augments T-type Ca^{2+} channel activity without changing channel surface density

Jin-Yong Park[1], Ho-Won Kang[1], Hyung-Jo Moon[1], Sung-Un Huh[1], Seong-Woo Jeong[3], Nikolai M. Soldatov[4] and Jung-Ha Lee[1,2]

[1]*Department of Life Science and* [2]*Interdisciplinary Program of Biotechnology, Sogang University, Shinsu-dong, Seoul 121-742, Korea*
[3]*Department of Physiology and Institute of Basic Medical Science, Yonsei University Wonju College of Medicine, Ilsan-Dong 162, Wonju, Kangwon-Do, Korea*
[4]*National Institute on Aging, 5600 Nathan Shock Drive, Baltimore, MD 21224, USA*

T-type Ca^{2+} channels play essential roles in numerous cellular processes. Recently, we reported that phorbol-12-myristate-13-acetate (PMA) potently enhanced the current amplitude of $Ca_v3.2$ T-type channels reconstituted in *Xenopus* oocytes. Here, we have compared PMA modulation of the activities of $Ca_v3.1$, $Ca_v3.2$ and $Ca_v3.3$ channels, and have investigated the underlying mechanism. PMA augmented the current amplitudes of the three T-type channel isoforms, but the fold stimulations and time courses differed. The augmentation effects were not mimicked by 4α-PMA, an inactive stereoisomer of PMA, but were abolished by preincubation with protein kinase C (PKC) inhibitors, indicating that PMA augmented T-type channel currents via activation of oocyte PKC. The stimulation effect on $Ca_v3.1$ channel activity by PKC was mimicked by endothelin when endothelin receptor type A was coexpressed with $Ca_v3.1$ in the *Xenopus* oocyte system. Pharmacological studies combined with fluorescence imaging revealed that the surface density of $Ca_v3.1$ T-type channels was not significantly changed by activation of PKC. The PKC effect on $Ca_v3.1$ was localized to the cytoplasmic II–III loop using chimeric channels with individual cytoplasmic loops of $Ca_v3.1$ replaced by those of $Ca_v2.1$.

(Received 18 July 2006; accepted after revision 25 September 2006; first published online 28 September 2006)
Corresponding author J.-H. Lee: Department of Life Science, Sogang University, Shinsu-dong, Seoul 121-742, Korea. Email: jhleem@sogang.ac.kr

A number of pivotal cellular effects have been attributed to T-type Ca^{2+} channels (T-channels) (Perez-Reyes, 2003; Yunker & McEnery, 2003). In thalamic neurons, T-type channels mediate neuronal burst firing and oscillatory behaviour by eliciting regenerative low threshold spikes (Huguenard, 1996). They are also involved in cardiac pacemaker activity (Hagiwara *et al.* 1988; Zhou & Lipsius, 1994; Chen *et al.* 2003), smooth muscle contraction (Xiong *et al.* 1995; Janssen, 1997), and hormone secretion (Matteson & Armstrong, 1986; Enyeart *et al.* 1993; Chen *et al.* 1999; Zhuang *et al.* 2000). Furthermore, calcium influx via T-channels is required for myoblast fusion (Bijlenga *et al.* 2000), neuritogenesis (Chemin *et al.* 2002), and the sperm acrosome reaction (Son *et al.* 2000). Cumulative evidence suggests that T-channels are implicated in the transmission of pain signals at both spinal and thalamic levels (Kim *et al.* 2003; Altier & Zamponi, 2004; Bourinet *et al.* 2005). Furthermore, abnormal expression of T-channels is responsible for pathological conditions such as cardiac hypertrophy and absence epilepsy (Tsakiridou *et al.* 1995; Martinez *et al.* 1999).

The electrophysiological and pharmacological features of T-channels have been extensively studied to establish how calcium influx via these channels affects these various cellular processes. Calcium entry through T-channels primarily causes depolarization of the plasma membrane, especially at the resting membrane potential around which they are activated because of their low threshold for activation. The subsequent rise of Ca^{2+} on the cytoplasmic side of the cell membrane can affect diverse downstream signalling molecules coupled to essential physiological functions (Perez-Reyes, 2003). T-channels are distinguished from high voltage-activated (HVA) Ca^{2+} channels by a number of criteria including channel activation and inactivation at relatively low voltage, transient current traces, slow deactivation, and tiny single channel conductance (Perez-Reyes, 2003). Recent molecular cloning and expression studies have demonstrated the existence of three T-channel gene isoforms: $Ca_v3.1$ (α_{1G}), $Ca_v3.2$ (α_{1H}) and $Ca_v3.3$ (α_{1I}) (Cribbs *et al.* 1998; Perez-Reyes *et al.* 1998; Lee *et al.* 1999).

T-channel activity, like that of most ion channels, can be modulated by hormones and neurotransmitters acting

 DOI: 10.1113/jphysiol.2006.117440

through signalling intermediates such as protein kinases A and C (Furukawa *et al.* 1992; Pemberton *et al.* 2000), calmodulin-dependent protein kinase II (Wolfe *et al.* 2002), tyrosine kinase (Arnoult *et al.* 1997), G-proteins (Wolfe *et al.* 2003) and lipid derivatives such as arachidonic acid (Zhang *et al.* 2000; Talavera *et al.* 2004). However, there has been controversy about the effect of protein kinase C (PKC) on T-channels: native T-currents have been variously reported to be up-regulated, down-regulated or unaffected by PKC. For example, T-currents in cultured neonatal rat ventricular myocytes were reported to be stimulated by 10 nM endothelin-1 (EDN1) via PKC, with stimulation antagonized by PKC inhibitors (Furukawa *et al.* 1992), whereas T-currents in rat dorsal root ganglion (DRG) neurons were reported to be inhibited by 10 nM PMA (Schroeder *et al.* 1990). Similar inhibition of T-currents by PKC activators has been reported in Purkinje cells from canine hearts, and in the clonal GH_3 line of anterior pituitary cells (Marchetti & Brown, 1988; Tseng & Boyden, 1991). On the other hand, PKC activators were also found to have no effect on T-currents in hippocampal neurons (O'Dell & Alger, 1991).

We recently showed that PMA strongly stimulates $Ca_v3.2$ channel activity via PKC in the *Xenopus* oocyte system (Park *et al.* 2003). In this present study, we compared activation of the three T-channel isoforms by PKC in the *Xenopus* oocyte system. PMA augmented $Ca_v3.1$, $Ca_v3.2$ and $Ca_v3.3$ channel current amplitudes to different extents, but did not affect other properties of the T-channel whole-cell currents. Subsequent examination revealed that the surface density of $Ca_v3.1$-EGFP was not significantly altered by activation of PKC and that the II–III cytoplasmic loop of $Ca_v3.1$ was responsible for PKC stimulation.

Methods

Preparation of cDNA constructs

The cloning of rat $Ca_v3.1$ (α_{1G}; AF027984) and human $Ca_v3.2$ (α_{1H}; AF051946) and $Ca_v3.3$ (α_{1I}; AF086827) has been previously described (Cribbs *et al.* 1998; Perez-Reyes *et al.* 1998; Lee *et al.* 1999). The cDNA encoding endothelin receptor type A (ET_A), in pcDNA3.1 was purchased from the Guthrie cDNA Resource Center. A PCR-based approach was used to make all the other constructs used in this work, and the PCR products were sequenced to confirm all sequences. In an attempt to improve the expression of constructs, we subcloned all the coding sequences into a high expression vector, pGEMHEA which contains the 5′ and 3′ untranslated regions of the *Xenopus* β globin gene.

The following constructs were made by overlap extension PCR, as originally described (Ho *et al.* 1989): $Ca_v3.1$-ΔN, $Ca_v3.1$-I/II, $Ca_v3.1$-II/III, $Ca_v3.1$-III/IV, and a series of point mutations. Double-stranded fragments were generated from the $Ca_v3.1$ cDNA or a partial $Ca_v2.1$ cDNA in two separate PCR amplifications, and fused subsequently in PCR reaction 3. For $Ca_v3.1$-ΔN, PCR reaction 1 used a general T7 primer and a unique reverse overlap primer (5′-GTTACAGACACGGGGCTGTCCCGACTC-3′). In PCR reaction 2, we used a forward primer that was the partial complement of the overlap primer used in PCR reaction 1 (5′-CAGCCCCGTGTCTGTAACCCGTGG-TTC-3′), and a reverse primer located within domain I (5′-GACTGCGGAGAAGCTGAC-3′), to generate the second fragment. The overlap sequences in the primers are underlined. When these two PCR products were mixed, denatured, and cooled, the complementary overlaps annealed and the junction was extended by DNA polymerase. Finally, the forward primer used in PCR reaction 1 and the reverse primer used in PCR reaction 2 amplified the fragment bearing the chimeric construct and the product was cloned into the original $Ca_v3.1$-pGEMHEA after a series of digestion and ligation steps, yielding construct $Ca_v3.1$-ΔN lacking amino acid residues 18–77. The point mutants were similarly made by overlap PCR using the following overlap primers to replace the serines putatively phosphorylated by PKC with alanines: S977/S979, 5′-AGGCTC**TGC**-CTC**AGC**CTTGGTGGCATCTCCCTC-3′ and 5′-ACC-AAG**GCT**GAG**GCA**GAGCCTGATTTCTTT-3′; S1027/S1031/S1032, 5′-GCT**GGCG**GCCTTGGGGTG**TGC**CAT-TGGTGTCGCAGC-3′ and 5′-**GCA**CACCCCAAG**GCC-GCC**AGCACAGGTGTGGGGGAA-3′; S1044/S1048/S1049, 5′-**GGCAGC**GGTACGTCG**AGCG**CCAGAGCC-CAGTGC-3′ and 5′-**GCT**CGACGTACC**GCTGCC**AGTGG-GTCCGCTGAG-3′; S1067/S1070/S1071, 5′-CGG**GGCG-GC**GCGGGC**AGCT**GGCGGACATTTCAT-3′ and 5′-CCA**GCT**GCCCGC**GCCGCC**CCGCACAGTCCCTGG-3′; S1084/S1087/S1088/S1091, 5′-**GGC**GTTCCT**GGC-GGC**GCGCCT**GGC**GGTCCAGCTGCTTGCCGC-3′ and 5′-**GCC**AGGCGC**GCCGCCA**GGAAC**GCC**CTGGGCC-GGGCCCCC-3′; S1097, 5′-CCGCTTTAG**GGC**GG-GGGCCCG**GCCCAG**-3′ and 5′-CGGGCCCCC**G-CC**CTAAAGCGGAGGAGC-3′. The overlap sequences are underlined with boldface letters corresponding to the mutated alanine residues. To create the chimeric constructs ($Ca_v3.1$-I/II, $Ca_v3.1$-II/III and $Ca_v3.1$-III/IV), DNAs encoding the intracellular loops connecting each domain of $Ca_v2.1$ were generated by RT-PCR from human brain total RNA (Invitrogen, Carlsbad, CA, USA). The PCR primers were designed from the human $Ca_v2.1$ sequence (GenBank accession number, NM023035): I/II loop, 5′-AAGGGCCCAACAACGGGATCA-3′ and 5′-GCGTGTTGAGAGCTACCAAAC-3′; II/III loop, 5′-TTTGGGAACTACACCCTCCTG-3′ and 5′-AGGA-CGAGCCCCAGGTCAATC-3′; III/IV loop, 5′-GTTCC-CCTTCTTCTTTGTCAA-3′ and 5′-AGCCCCATAG-AACTTCATCAT-3′. The PCR products were subcloned into TOPO TA vector (Invitrogen, Carlsbad, CA, USA),

verified by sequencing, and used for the overlap PCR. The resulting chimeric constructs consist of the entire $Ca_v3.1$ except for the substitution of intracellular loops with the corresponding regions of $Ca_v2.1$.

A carboxyl-terminal deletion mutant ($Ca_v3.1$-ΔC) lacking amino acid residues 1827–2254 was constructed by introducing a stop codon (TAA) proximal to the C-terminus using standard PCR. The N-loop and II–III loops of $Ca_v3.1$ were produced by PCR and subcloned into pGEMHEA vector. For the green fluorescence experiment, the $Ca_v3.1$ 3′ untranslated region was removed and the coding sequence of EGFP (enhanced green fluorescence protein) fused to the C-terminus (BD Biosciences Clontech).

Imaging

Surface expression of EGFP-tagged $Ca_v3.1$ before and 30 min after application of PMA was examined by laser scanning microscopy (LSM 5 Pascal, Zeiss, Germany). Line intensities of fluorescence images across oocyte membrane were generated using Metamorph (Universal Imaging), and exhibited as arbitrary units of pixel density. Arbitrary units obtained were compared before and after PKC stimulation by PMA.

Chemicals

A stock solution of 50 μM kurtoxin (Peptide Institute, Osaka, Japan) was prepared in distilled water. All other chemicals were from Sigma (St Louis, MO, USA) and were prepared as concentrated stock solutions in DMSO, stored frozen at -20°C and diluted as desired in recording solution.

Expression of cDNA constructs in *Xenopus* oocytes

The cDNA constructs were linearized at their 3′ ends by AflII. Transcripts were synthesized *in vitro* using T7 RNA polymerase according to the manufacturer's protocol (Ambion, Austin, TX, USA), and the concentrations of the synthesized cRNAs were measured spectrophotometrically.

Oocytes were obtained from female *Xenopus laevis* (Nasco, WI, USA) using a standard procedure, which was approved by the Sogang University Animal Care Committee. Frogs were anaesthetized using 3-aminobenzoic acid (1 g l^{-1}, Sigma), then oocytes were collected by making a 1 cm incision in the ventral abdomen and removing a portion of the ovary. The frog was sutured and allowed to recover for 1–2 h before returning it to the culture tank. Oocytes were prepared for microinjection as previously described (Park *et al.* 2003). Briefly, several ovary lobes were surgically removed from mature female *Xenopus laevis* and torn into small clusters in standard oocyte saline (SOS) solution (mM: 100 NaCl, 2 KCl, 1.8 $CaCl_2$, 1 $MgCl_2$, 5 Hepes, 2.5 pyruvic acid, 50 μg ml^{-1} gentamicin, pH 7.6). The follicular membranes were removed by digestion in Ca^{2+}-free OR2 solution (mM: 82.5 NaCl, 2.5 KCl, 1 $MgCl_2$, 5 Hepes, pH 7.6) containing 2 mg ml^{-1} collagenase (Sigma). Oocytes were injected under a stereomicroscope with 2–20 ng of cRNA using a Drummond Nanoject pipette injector (Parkway, PA, USA) attached to a Narishige micromanipulator (Tokyo, Japan).

Electrophysiological recordings and data analysis

Barium currents were measured at room temperature 4–8 days after cRNA injection using a two-electrode voltage-clamp amplifier (OC-725C, Warner Instruments, Hamden, CT, USA). Microelectrodes (Warner Instruments) were filled with 3 M KCl and their resistances were 0.2–1.0 MΩ. The 10 mM Ba^{2+} bath solution contained (mM): 10 $Ba(OH)_2$, 90 NaOH, 1 KOH, 5 Hepes (pH 7.4 with methanesulphonic acid). The currents were sampled at 5 kHz and low pass filtered at 1 kHz using the pCLAMP system (Digidata 1320A and pCLAMP 8; Axon Instruments, Union City, CA, USA). Peak currents and exponential fits to currents were analysed using Clampfit software (Axon Instruments) and presented graphically using Prism software (GraphPad, San Diego, CA, USA). Data are given as means $\pm$ S.E.M., and were tested for significance by one-way analysis of variance (ANOVA) followed by post tests and a two-tailed unpaired *t* test with $P < 0.05$, $P < 0.01$ and $P < 0.001$ as levels of significance.

Results

The $Ca_v3.1$, $Ca_v3.2$, or $Ca_v3.3$ T-type Ca^{2+} channels expressed in *Xenopus* oocytes generated robust inward currents evoked by a test potential of -20 mV from a holding potential of -90 mV. During a series of depolarizing voltage steps, the threshold potential for activation of the three T-channels was around -60 mV, peak currents were obtained at -20 mV, and reversal potentials were around $+40$ mV. As reported (Cribbs *et al.* 1998; Perez-Reyes *et al.* 1998; Lee *et al.* 1999), the $Ca_v3.1$ and $Ca_v3.2$ T-channel currents were characterized by fast activating and inactivating kinetics, whereas the $Ca_v3.3$ T-channel current displayed slowly activating and inactivating kinetics. We chose oocytes yielding peak current amplitudes of about 0.5 μA to study PKC-dependent regulation in order to obtain proper control of voltage clamping.

We have previously shown that $Ca_v3.2$ channels expressed in *Xenopus* oocytes are potently up-regulated

via endogenous PKC in response to phorbol-12-myristate-13-acetate (PMA) (Park *et al.* 2003). In the present study, we compared the effects of PMA on all three Ca_v3 isoforms. When T-type currents were repeatedly evoked by a test potential of −20 mV every 20 s without applying PMA, their amplitude was stable without significant run-up or run-down over periods of up to 30 min. To see how each channel was modulated by PKC, we applied 100 nM PMA to a chamber containing an oocyte expressing one or other of the three T-channels. Representative T-current traces recorded before and 15 min after application of PMA are overlapped in Fig. 1*A*, showing that the activities of all three channels were greatly enhanced by PMA.

PMA increased the Ca_v3 current amplitudes in a concentration-dependent manner, and fitting the data to the Hill equation gave estimated EC_{50} values for $Ca_v3.1$, $Ca_v3.2$ and $Ca_v3.3$ of 21.0 ± 1.1, 10.8 ± 1.1 and 3.2 ± 1.2 nM, respectively, and Hill coefficients for $Ca_v3.1$, $Ca_v3.2$ and $Ca_v3.3$ of 1.4 ± 0.1, 1.7 ± 0.2 and 0.9 ± 0.1, respectively ($n = 5$–8) (Fig. 1*B*). Stimulation almost saturated at 100 nM PMA and we used this concentration to evoke maximal currents in the following experiments.

Superfusion of 100 nM PMA onto oocytes expressing $Ca_v3.1$, $Ca_v3.2$ or $Ca_v3.3$ similarly induced increases in current amplitude after a lag period of 2–3 min (Fig. 1*C*). However, the fold stimulations and time courses of the stimulations differed. The maximum fold stimulations of the $Ca_v3.1$, $Ca_v3.2$ and $Ca_v3.3$ currents over 15 min were 2.67 ± 0.15 ($n = 51$), 2.40 ± 0.16 ($n = 29$) and 3.53 ± 0.25 ($n = 25$), respectively (Fig. 1*C*). The activities

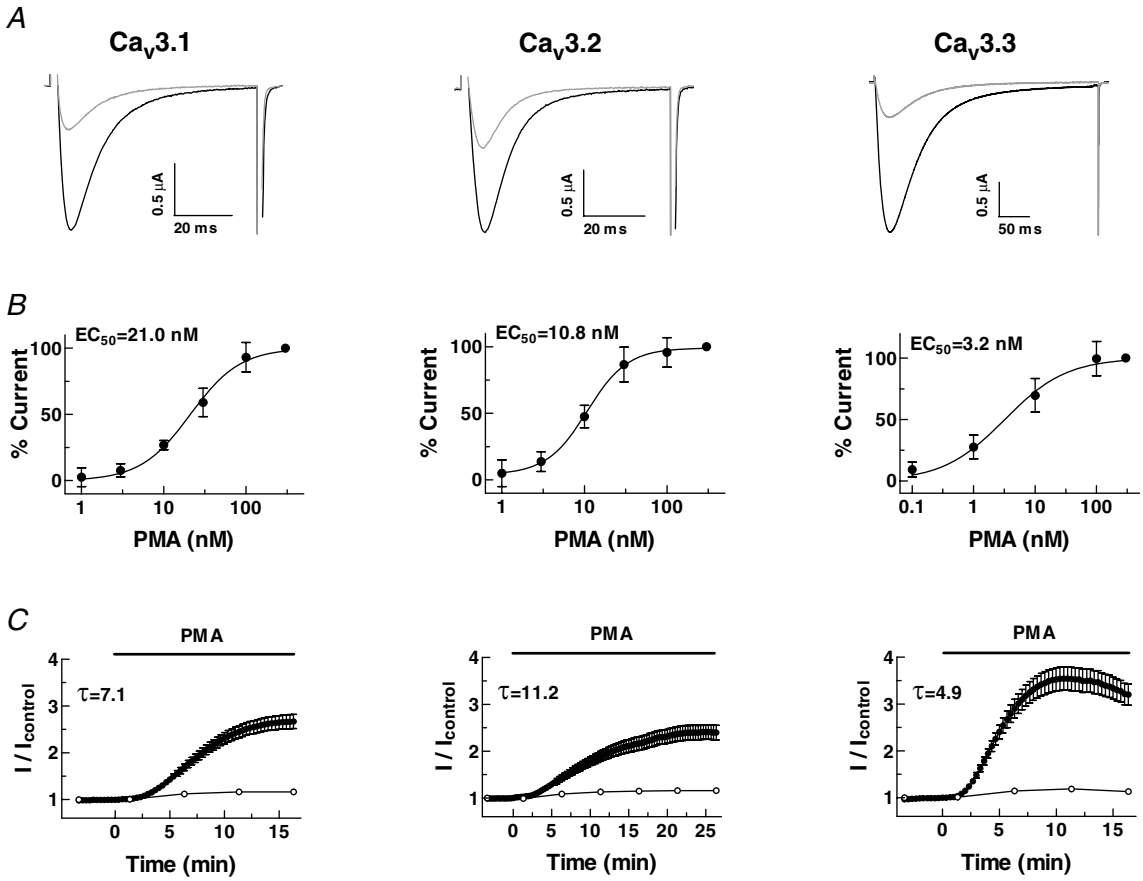

Figure 1. Effect of PMA on Ca_v3 currents expressed in *Xenopus* oocytes
Recombinant Ca_v3 channels were expressed in *Xenopus* oocytes and their currents were measured in a solution containing 10 mM Ba^{2+} as charge carrier. Oocytes were held at −90 mV and depolarized to a test potential of −20 mV. *A*, representative current traces taken before (grey) and 15 min after (black) 100 nM PMA treatment ($Ca_v3.1$, $Ca_v3.2$ and $Ca_v3.3$, respectively). *B*, concentration–response relationships for PMA in oocytes expressing $Ca_v3.1$, $Ca_v3.2$, $Ca_v3.3$ channels. The currents were normalized with that elicited by 300 nM PMA. The smooth curve was derived by fitting the data to the Hill equation (EC_{50} = $Ca_v3.1$, 21.0 ± 1.1 nM; $Ca_v3.2$, 10.8 ± 1.1 nM; $Ca_v3.3$, 3.2 ± 1.2 nM; $n = 4$–8). *C*, time course of the effect of PMA on peak currents at −20 mV (●) and on capacitance (○). The stimulations of the three T-currents fitted to a one-phase single exponential association equation, where τ is the time constant. Data are means ± S.E.M.

Table 1. Summary of the electrophysiological properties of the T-type channels before and after stimulation by PMA

		$V_{50,Act}$ (mV)	$V_{50,Inact}$ (mV)	$\tau_{recovery}$ (ms)
$Ca_v3.1$	Control	-40.0 ± 0.8 ($n = 10$)	-64.9 ± 0.7 ($n = 11$)	92.2 ± 5.9 ($n = 10$)
	PMA	-41.9 ± 0.9 ($n = 10$)	-66.1 ± 0.8 ($n = 11$)	102.9 ± 7.4 ($n = 10$)
$Ca_v3.2$	Control	-36.2 ± 0.6 ($n = 10$)	-62.0 ± 0.9 ($n = 11$)	248.5 ± 24.9 ($n = 7$)
	PMA	-36.1 ± 0.6 ($n = 10$)	-61.9 ± 0.8 ($n = 11$)	266.7 ± 15.3 ($n = 7$)
$Ca_v3.3$	Control	-29.1 ± 1.3 ($n = 11$)	-55.6 ± 0.9 ($n = 11$)	203.2 ± 5.9 ($n = 8$)
	PMA	-31.9 ± 1.5 ($n = 11$)	-54.6 ± 1.4 ($n = 11$)	197.7 ± 11.1 ($n = 8$)

Voltage dependence (V_{50}) was estimated from the smooth Boltzmann curve fitted to the data points. Single exponential curves were fitted to the recovery from inactivation. Data shown are means ± S.E.M. Numbers of oocytes tested are given in parentheses.

of the $Ca_v3.1$ and $Ca_v3.2$ channels increased for up to ~30 min and remained stable thereafter or sometimes fell slightly, whereas that of the $Ca_v3.3$ channel reached a maximum within 10 min, and slowly declined thereafter. The stimulation data were fitted by a single exponential equation, given that the time constants (τ) for $Ca_v3.1$, $Ca_v3.2$ and $Ca_v3.3$ are 7.1, 11.2 and 4.9, respectively. When oocytes expressing the three T-type channels were washed after reaching their maximal stimulations, the $Ca_v3.1$ and $Ca_v3.2$ currents were partially recovered (10–20%), and the $Ca_v3.3$ currents were to a large extent recovered ($80 \pm 10\%$, $n = 5$) over 30 min.

To see whether any change of plasma membrane surface area is involved in the PMA-mediated channel stimulation, we recorded cell membrane capacitance, which reflects cell membrane surface area, at the same time as channel currents (Vasilets *et al.* 1990). Despite the marked enhancement of T-channel current amplitudes by PMA, there was no significant change in capacitance in any of the oocytes examined (Fig. 1*C*).

We next tested whether the current–voltage relationships, activation curves, steady-state inactivation curves, and recovery from inactivation of the three T-channel whole-cell currents were modulated by application of PMA. Although PMA induced large increases in current amplitudes at all the potentials tested, it did not significantly affect current–voltage relationships (Fig. 2*A*) or the activation or inactivation curves (Fig. 2*B*). Consistently, the potentials of half-activation ($V_{50,Act}$) and inactivation ($V_{50,Inact}$) were unchanged (Table 1). In addition, PMA did not affect the recovery from inactivation of any of the channels (Fig. 2*C* and Table 1). These results indicate that, except for current amplitude, none of the electrophysiological properties were significantly affected by PMA treatment.

In order to test whether the PMA-induced T-channel stimulation was mediated by activation of PKC, we first examined whether 4α-PMA, an inactive stereoisomer of PMA, can stimulate peak current amplitude of T-channels expressed in oocytes. As shown in Fig. 3, this inactive analogue (100 nM) had no significant effect ($Ca_v3.1$, 1.05 ± 0.10; $Ca_v3.2$, 1.04 ± 0.03; $Ca_v3.3$, 1.02 ± 0.09 fold).

We then enquired whether PKC inhibitors, such as chelerythrine and bisindolylmaleimide (Herbert *et al.* 1990; Toullec *et al.* 1991), abrogated the PMA responses. Preincubation of oocytes in 20 μM chelerythrine greatly attenuated the stimulation of $Ca_v3.1$, $Ca_v3.2$ and $Ca_v3.3$ currents in response to 100 nM PMA (Fig. 3), and preincubation with 5 μM bisindolylmaleimide totally abolished stimulation (Fig. 3). These results strongly support the view that PMA stimulates recombinant T-channel current activity via activation of endogenous PKC in oocytes.

To reconstitute a physiological second messenger pathway, the $Ca_v3.1$ channel was coexpressed with endothelin receptor type A (ET_A) in *Xenopus* oocytes, because activation of the endothelin receptor is known to be coupled with cascades of G_q protein, phospholipase C and PKC activation. Expression of ET_A in oocytes was confirmed by measuring endogenous Cl^- currents evoked by inositol-3-phosphate-mediated Ca^{2+} release from internal stores in response to 10 nM EDN1 (Dascal, 1987; Fig. 4*A*), and possible contamination of these Ca^{2+}-dependent Cl^- currents was prevented by injecting BAPTA (50 mM; 50 nl) into the oocytes 30 min before recording $Ca_v3.1$ currents. Application of 10 nM EDN1 caused a 2.34 ± 0.28 fold stimulation of $Ca_v3.1$ currents with a time course similar to the PMA-induced stimulation (Fig. 4*B* and *C*). EDN1 did not alter $Ca_v3.1$ currents in oocytes in which ET_A was not coexpressed with the T-channel (Fig. 4*C*).

To explore the mechanism of PKC stimulation, we tested whether PMA increases the surface density of T-channel proteins. $Ca_v3.1$ channels were tagged with enhanced green fluorescence protein (EGFP), and their fluorescence was measured with a confocal microscope. Application of PMA to oocytes expressing EGFP-$Ca_v3.1$ enhanced current amplitude but did not cause any detectable change of EGFP fluorescence (Pre-PMA, 68.8 ± 6.6; Post-PMA, 69.0 ± 7.4 arbitrary units, $n = 5$) (Fig. 5*A*). We also used

kurtoxin, a T-channel blocker (Chuang *et al.* 1998), to test for PMA-induced surface expression of $Ca_v3.1$ channels. Application of kurtoxin (300 nM) strongly inhibited $Ca_v3.1$ currents and these hardly recovered at all when the toxin was washed out (Fig. 5*B*). If the PKC augmentation of $Ca_v3.1$ currents was due to increased expression in the membrane via trafficking, PMA should lead to transport of new $Ca_v3.1$ channels into the plasma membrane regardless of the inhibition of the existing channels, thereby increasing channel activity. However, PMA did not significantly reverse the inhibition by kurtoxin (wash, 0.34 ± 0.15; PMA, 0.49 ± 0.20 fold). Overall, these results suggest that the PKC stimulation of $Ca_v3.1$ currents is not due to increased channel density.

To localize the region(s) of the $Ca_v3.1$ responsible for the PKC-dependent enhancement, we created channel loop

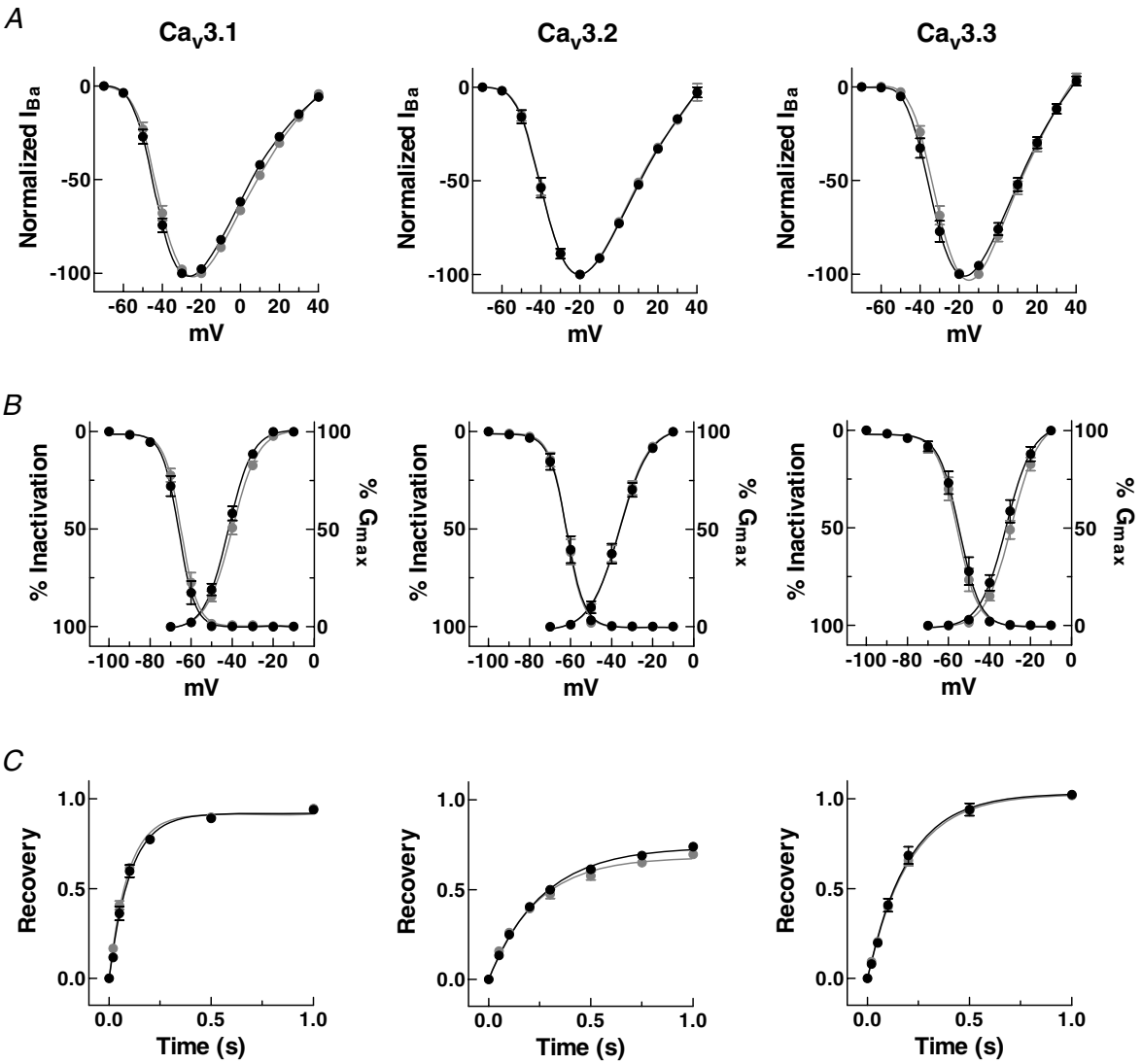

Figure 2. Electrophysiological properties of Ca_v3 currents before and after application of PMA
A, current–voltage relationships. Peak currents evoked by test potentials of different voltages were normalized to the maximum observed in each experimental condition (before, grey; after application of PMA, black). *B*, activation and steady-state inactivation. Activation curves were obtained by the chord conductance method, where conductance (G) was calculated by dividing current amplitude by the driving force (observed reversal potential minus the test potential). The data for each cell were normalized to the maximum observed in that cell. Channel availability was tested during voltage steps to −20 mV after 10 s prepulses of varying potentials. The data were normalized to the maximum current observed after prepulse to −100 mV, averaged, and fitted. Smooth curves represent the fit to the data with the Boltzmann equation ($G = 1/[1 + \exp(V_{50} - V)/k]$), where V_{50} is the half-activation voltage, and k is a slope factor. *C*, recovery from inactivation. Relative peak currents of the test pulse are plotted as a function of interpulse duration. The relationships were fitted by single exponential association. Data represent means ± S.E.M. ($n = 7$–11).

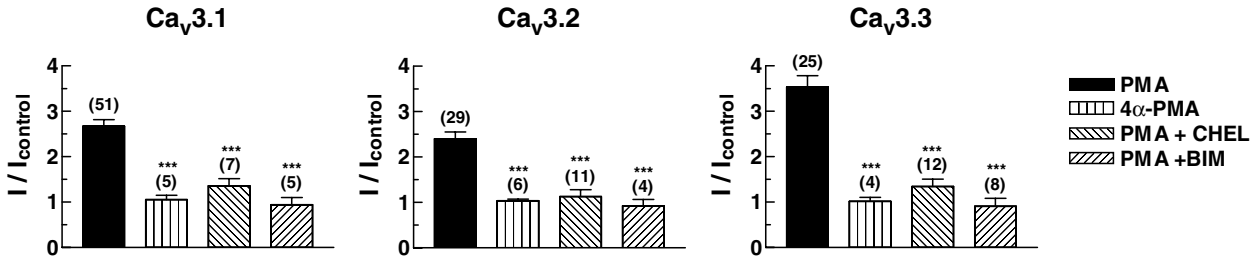

Figure 3. Specificity of the PMA response
Treatments were: PMA (100 nM); 4α-PMA (100 nM); chelerythrine (CHEL, 20 μM); bisindolylmaleimide (BIM, 5 μM). The inactive analogue of PMA, 4α-PMA did not mimic the stimulatory effect of PMA. Preincubation with the PKC inhibitors CHEL and BIM strongly reduced stimulation. Numbers in parentheses are the number of oocytes tested in each experiment. Data are means ± S.E.M. ***$P \leq 0.001$ compared with PMA alone.

chimeras by replacing individual cytoplasmic loops of $Ca_v3.1$ with the corresponding loops of $Ca_v2.1$, whose activity is insensitive to activation by PKC (Stea *et al.* 1995). Involvement of the N- or C-terminus of the $Ca_v3.1$ was also examined by constructing truncations of $Ca_v3.1$ lacking the N- or C-terminal tail (Fig. 6*A*). The fold stimulation of $Ca_v3.1$-II/III in response to 100 nM PMA for 15 min was 0.82 ± 0.10, compared to those of $Ca_v3.1$-ΔN, $Ca_v3.1$-ΔC, $Ca_v3.1$-I/II and $Ca_v3.1$-III/IV of 2.63 ± 0.48, 2.37 ± 0.15, 2.40 ± 0.30 and 2.27 ± 0.13 fold, respectively ($n = 4$–9, Fig. 6*A*). These data imply that loop II–III plays a crucial role in PKC-mediated stimulation.

We tested the validity of this conclusion by over-expressing the II–III loop, which might be expected to mask the PKC effect on $Ca_v3.1$. As expected, over-expression of loop II–III almost inhibited the PKC stimulation (Fig. 6*B*). On the whole, overexpression of the N-terminal tail did not affect the PKC stimulation. Taken together, these findings suggest that loop II–III contains essential structural element(s) required for the PKC effect, such as a PKC phosphorylation site(s).

Discussion

PKCs are a ubiquitously expressed family of kinases that phosphorylate a myriad of target proteins including ion channels, thereby regulating multiple cellular processes (Murray *et al.* 1994, 1997; Newton, 1995; Stea *et al.* 1995; Yamazaki *et al.* 1999; Dempsey *et al.* 2000; Lan *et al.* 2001). Studies of PKC-dependent modulation of native T-currents have yielded conflicting results. For example, PKC activation in neonatal rat ventricular myocytes potentiated T-currents (Furukawa *et al.* 1992), while reducing T-currents in rat DRG neurons (Schroeder *et al.* 1990), canine Purkinje cells (Tseng & Boyden, 1991) and GH_3 cells (Marchetti & Brown, 1988). In addition, PKC activators did not significantly affect T-channel activity in hippocampal neurons (O'Dell & Alger, 1991). The cloning of the T-type channels allowed us to re-examine this issue in the *Xenopus* oocyte expression system.

We showed above that PKC activation strongly stimulated whole-cell Ba^{2+} currents via all three T-channels expressed in the oocyte system. However, analysis of the stimulation revealed different time constants of the three channels (Fig. 1). There was no apparent change in the voltage dependence of gating as reflected by the activation curve, the steady-state inactivation curve, or recovery from inactivation

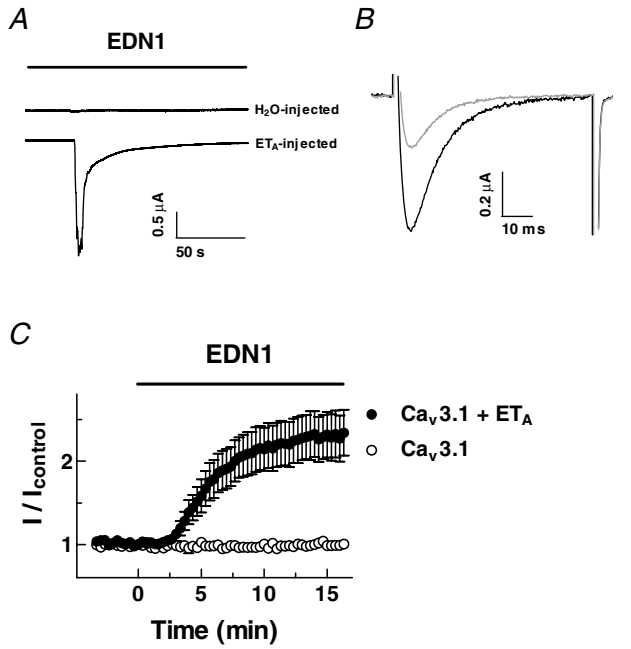

Figure 4. Reconstitution of endothelin-1-induced modulation of $Ca_v3.1$ T-type channel activity in *Xenopus* oocytes
A, typical chloride currents recorded in response to 10 nM endothelin-1 (EDN1) from oocytes injected with either H_2O or endothelin receptors (ET_A). Currents were measured in a solution containing 10 mM Ba^{2+}, in the absence of Ca^{2+} chelators. *B*, currents were recorded in oocytes expressing $Ca_v3.1$ and ET_A before (grey) and 15 min after the application of EDN1 (black). To prevent contamination by Cl^- currents, oocytes were injected with BAPTA. *C*, time course of changes in fold stimulation of $Ca_v3.1$ currents by EDN1. Oocytes were injected with $Ca_v3.1$ cRNA of channels alone and cRNA of channels and ET_A. Data are means ± S.E.M. ($n = 4$–10).

(Fig. 2); the only parameter altered was G_{max} (maximal macroscopic conductance). Similarly, studies of PKC modulation of L-type Ca^{2+} channels (Singer-Laha *et al.* 1992; McHugh *et al.* 2000), Na^+ channels (Murray *et al.* 1997), and K^+ channels (Murray *et al.* 1994; Peretz *et al.* 1996; Mao *et al.* 2004) did not find any changes of voltage dependence. Our pharmacological studies combined with fluorescence imaging showed that the number of channels on the surface of oocytes expressing $Ca_v3.1$ was not altered by PKC. These findings rule out the possibility that the PKC stimulation of T-channel amplitude results from increased channel trafficking to the cell surface (Lan *et al.* 2001; Sun *et al.* 2003). We therefore propose that PKC transforms non-functional forms of T-channels to functional forms permeable to Ba^{2+}, as suggested for the MinK potassium channel (Blumenthal & Kaczmarek, 1994).

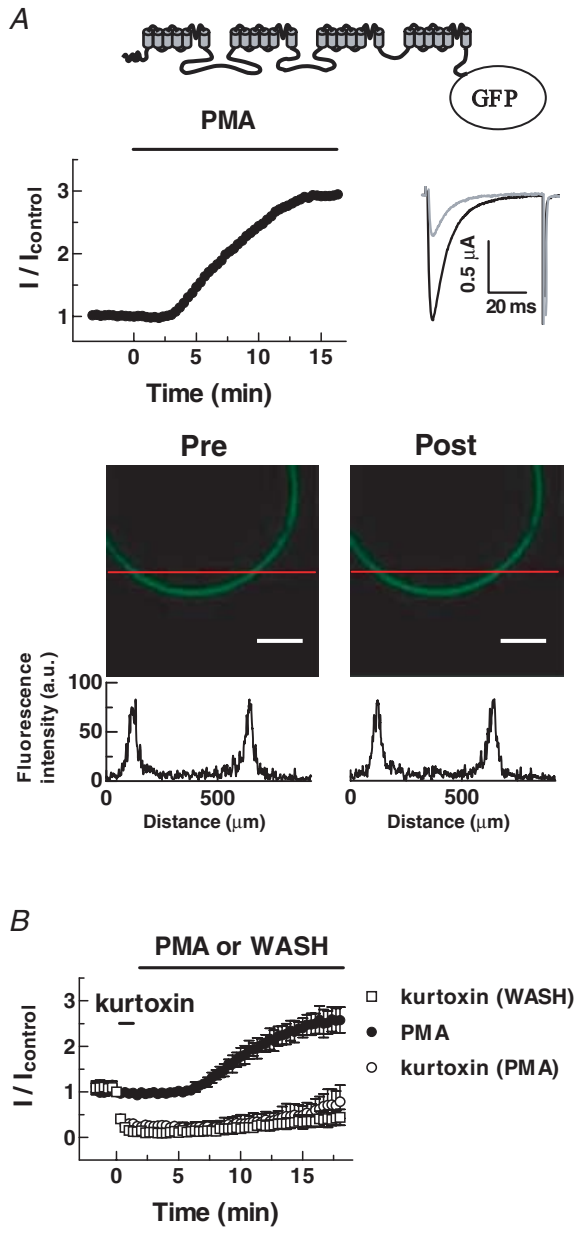

Figure 5. PMA does not alter the surface expression of $Ca_v3.1$
A, upper panels, schematic representation of the EGFP-fused $Ca_v3.1$ channel. Time course of the PMA effect on the peak current amplitude of GFP-$Ca_v3.1$ and representative current traces before (grey) and after (black) PMA treatment. Lower panels, confocal images of fluorescence of oocytes expressing EGFP-$Ca_v3.1$. Representative line fluorescence intensities across membrane portions were represented as arbitrary units below the confocal images. The experiments were repeated 5 times with similar results. Scale bars, 200 μm. *B*, time course showing that PMA does not accelerate recovery from the inhibitory effect of kurtoxin (300 nM). Data are means ± S.E.M. ($n = 4$–5).

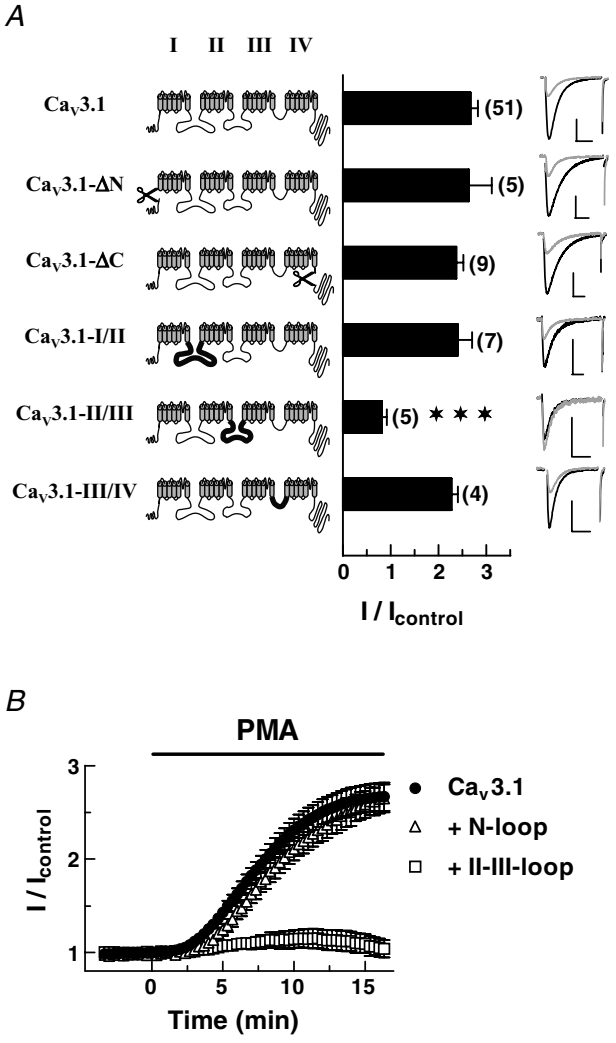

Figure 6. The critical role of intracellular loop II–III in PKC stimulation
A, schematic representations of the α_1-subunits of: wild-type Ca^{2+} channels, truncation mutants and chimeric mutants in which the I–II, II–III, or III–IV loops of $Ca_v3.1$ were replaced by those of $Ca_v2.1$. Data are means ± S.E.M. The number of oocytes tested is given in parentheses. $^{***}P \leq 0.001$ compared with WT. *B*, time course of PKC modulation of $Ca_v3.1$ currents recorded from oocytes coinjected with the N-terminal or the II–III loop of $Ca_v3.1$. Peak currents were normalized to the control, and plotted as a function of time.

The structural region crucial for PKC regulation was localized to the II–III loop of $Ca_v3.1$. We tested possible involvement of Ser977, Ser979, Ser1027, Ser1031 and Ser1032 by individually mutating them into Ala, because these sites are found in the motifs, $Arg(Lys)X_{0-2}Thr/SerX_{0-2}Arg(Lys)$, known to be phosphorylated by PKC (Kennelly & Krebs, 1991). All of the five mutant channels were stimulated by PMA and their stimulation profiles were similar to that of wild-type $Ca_v3.1$, suggesting that these sites may not contribute to the PKC-mediated stimulation. In addition to the three sites examined, there are 39 more putative sites fitting the consensus motifs for PKC phosphorylation. Their involvement(s) remains to be investigated by making individual point mutations.

Although direct phosphorylation of $Ca_v3.1$ by PKC is a candidate mechanism underlying the PKC-mediated stimulation, it is also possible that PKC stimulation is an indirect consequence of phosphorylation of associated targeting, anchoring, or signalling protein(s), as proposed for NMDA channels (Zheng *et al.* 1999). The intracellular II–III loops of voltage-dependent calcium channel α_1-subunits have been shown to be important for interaction with other signalling effectors. In skeletal muscle, excitation–contraction coupling is thought to proceed through protein–protein interactions between the dihydropyridine-sensitive voltage-gated calcium channel and the ryanodine receptor calcium release channel, with the intracellular II–III loop as linker (Tanabe *et al.* 1990; Catterall, 1991). The interaction of SNARE (soluble *N*-ethylmaleimide-sensitive factor attached protein receptor) with a synaptic protein interaction site on the II–III loop of the Ca_v2 family is another example (Sheng *et al.* 1994). Recent studies of T-type channels suggest that the II–III loop may serve as a centre for integrating multiple signalling pathways via G-protein $\beta\gamma$-subunits and Ca^{2+}–calmodulin-dependent kinase II (Welsby *et al.* 2003; Wolfe *et al.* 2003). Taken together with these previous findings, our observations suggest that the II–III loop of T-type channels contains structural elements required for regulating channel activity via diverse signalling pathways.

There are contradictory findings concerning PKC modulation of T-channel activity, and the PKC-dependent modulation profiles of T-channels appear to depend on the expression system used. What causes the differential modulation of T-channel activity by PKC depending on the system? There appear to be at least three possibilities. First, the expression or activation of endogenous PKC isozymes may be system dependent. The remarkable heterogeneity of PKC signal transduction pathways supports this scenario (Dempsey *et al.* 2000), and it gains further support from evidence for PKC isozyme-specific regulation of ion channel activity (Xiao *et al.* 2001, 2003; Chen *et al.* 2005). Hence, the particular isozymes responsible for the PKC effects on T-channel activity in different expression systems need to be identified. Next, PKC modulation of T-channels may involve PKC-interacting proteins, as shown for $Ca_v2.2$ channels (Maeno-Hikichi *et al.* 2003). Such PKC-interacting proteins confer specificity on individual PKC isozymes by regulating their activity and cellular location, and endow these isozymes with the ability to perform specific cellular functions (Poole *et al.* 2004). Finally, unidentified proteins, such as T-channel β-subunits, specifically associated with T-channels, may be crucial for system-specific modulation. Future investigations aimed at isolating protein(s) that interact with T-channels may clarify this matter.

References

Altier C & Zamponi GW (2004). Targeting Ca^{2+} channels to treat pain: T-type versus N-type. *Trends Pharmacol Sci* **25**, 465–470.

Arnoult C, Lemos JR & Florman HM (1997). Voltage-dependent modulation of T-type calcium channels by protein tyrosine phosphorylation. *EMBO J* **16**, 1593–1599.

Bijlenga P, Liu JH, Espinos E, Haenggeli CA, Fischer-Lougheed J, Bader CR & Bernheim L (2000). T-type α_{1H} Ca^{2+} channels are involved in Ca^{2+} signaling during terminal differentiation (fusion) of human myoblasts. *Proc Natl Acad Sci U S A* **97**, 7627–7632.

Blumenthal EM & Kaczmarek LK (1994). The minK potassium channel exists in functional and nonfunctional forms when expressed in the plasma membrane of *Xenopus* oocytes. *J Neurosci* **14**, 3097–3105.

Bourinet E, Alloui A, Monteil A, Barrere C, Couette B, Poirot O, Pages A, McRory J, Snutch TP, Eschalier A & Nargeot J (2005). Silencing of the $Ca_v3.2$ T-type calcium channel gene in sensory neurons demonstrates its major role in nociception. *EMBO J* **24**, 315–324.

Catterall WA (1991). Excitation-contraction coupling in vertebrate skeletal muscle: a tale of two calcium channels. *Cell* **64**, 871–874.

Chemin J, Nargeot J & Lory P (2002). Neuronal T-type α_{1H} calcium channels induce neuritogenesis and expression of high-voltage-activated calcium channels in the NG108-15 cell line. *J Neurosci* **22**, 6856–6862.

Chen XL, Bayliss DA, Fern RJ & Barrett PQ (1999). A role for T-type Ca^{2+} channels in the synergistic control of aldosterone production by ANG II and K^+. *Am J Physiol Renal Physiol* **276**, F674–F683.

Chen Y, Cantrell AR, Messing RO, Scheuer T & Catterall WA (2005). Specific modulation of Na^+ channels in hippocampal neurons by protein kinase Cε. *J Neurosci* **25**, 507–513.

Chen CC, Lamping KG, Nuno DW, Barresi R, Prouty SJ, Lavoie JL, Cribbs LL, England SK, Sigmund CD, Weiss RM, Williamson RA, Hill JA & Campbell KP (2003). Abnormal coronary function in mice deficient in α_{1H} T-type Ca^{2+} channels. *Science* **302**, 1416–1418.

Chuang RS, Jaffe H, Cribbs L, Perez-Reyes E & Swartz KJ (1998). Inhibition of T-type voltage-gated calcium channels by a new scorpion toxin. *Nat Neurosci* **1**, 668–674.

Cribbs LL, Lee J-H, Yang J, Satin J, Zhang Y, Daud A, Barclay J, Williamson MP, Fox M, Rees M & Perez-Reyes E (1998). Cloning and characterization of α_{1H} from human heart, a member of the T-type Ca^{2+} channel gene family. *Circ Res* **83**, 103–109.

Dascal N (1987). The use of *Xenopus* oocytes for the study of ion channels. *CRC Crit Rev Biochem* **22**, 317–387.

Dempsey EC, Newton AC, Mochly-Rosen D, Fields AP, Reyland ME, Insel PA & Messing RO (2000). Protein kinase C isozymes and the regulation of diverse cell responses. *Am J Physiol Lung Cell Mol Physiol* **279**, L429–L438.

Enyeart JJ, Mlinar B & Enyeart JA (1993). T-type Ca^{2+} channels are required for adrenocorticotropin-stimulated cortisol production by bovine adrenal zona fasciculata cells. *Mol Endocrinol* **7**, 1031–1040.

Furukawa T, Ito H, Nitta J, Tsujino M, Adachi S, Hiroe M, Marumo F, Sawanobori T & Hiraoka M (1992). Endothelin-1 enhances calcium entry through T-type calcium channels in cultured neonatal rat ventricular myocytes. *Circ Res* **71**, 1242–1253.

Hagiwara N, Irisawa H & Kameyama M (1988). Contribution of two types of calcium currents to the pacemaker potentials of rabbit sino-atrial node cells. *J Physiol* **395**, 233–253.

Herbert JM, Augereau JM, Gleye J & Maffrand JP (1990). Chelerythrine is a potent and specific inhibitor of protein kinase C. *Biochem Biophys Res Commun* **172**, 993–999.

Ho SN, Hunt HD, Horton RM, Pullen JK & Pease LR (1989). Site-directed mutagenesis by overlap extension using the polymerase chain reaction. *Gene* **77**, 51–59.

Huguenard JR (1996). Low-threshold calcium currents in central nervous system neurons. *Annu Rev Physiol* **58**, 329–348.

Janssen J (1997). T-type and L-type Ca^{2+} currents in canine bronchial smooth muscle: characterization and physiological roles. *Am J Physiol Cell Physiol* **272**, C1757–C1765.

Kennelly PJ & Krebs EG (1991). Consensus sequences as substrate specificity determinants for protein kinases and protein phosphatases. *J Biol Chem* **266**, 15555–15558.

Kim D, Park D, Choi S, Lee S, Sun M, Kim C & Shin HS (2003). Thalamic control of visceral nociception mediated by T-type Ca^{2+} channels. *Science* **302**, 117–119.

Lan JY, Skeberdis VA, Jover T, Grooms SY, Lin Y, Araneda RC, Zheng X, Bennett MV & Zukin RS (2001). Protein kinase C modulates NMDA receptor trafficking and gating. *Nat Neurosci* **4**, 382–390.

Lee JH, Daud AN, Cribbs LL, Lacerda AE, Pereverzev AP, Klockner U, Schneider T & Perez-Reyes E (1999). Cloning and expression of a novel member of the low voltage-activated T-type calcium channel family. *J Neurosci* **19**, 1912–1921.

McHugh D, Sharp EM, Scheuer T & Catterall WA (2000). Inhibition of cardiac L-type calcium channels by protein kinase C phosphorylation of two sites in the N-terminal domain. *Proc Natl Acad Sci U S A* **97**, 12334–12338.

Maeno-Hikichi Y, Chang S, Matsumura K, Lai M, Lin H, Nakagawa N, Kuroda S & Zhang JF (2003). A PKCε-ENH-channel complex specifically modulates N-type Ca^{2+} channels. *Nat Neurosci* **6**, 468–475.

Mao J, Wang X, Chen F, Wang R, Rojas A, Shi Y, Piao H & Jiang C (2004). Molecular basis for the inhibition of G protein-coupled inward rectifier K^+ channels by protein kinase C. *Proc Natl Acad Sci U S A* **101**, 1087–1092.

Marchetti C & Brown AM (1988). Protein kinase activator 1-oleoyl-2-acetyl-sn-glycerol inhibits two types of calcium currents in GH3 cells. *Am J Physiol Cell Physiol* **254**, C206–C210.

Martinez ML, Heredia MP & Delgado C (1999). Expression of T-type Ca^{2+} channels in ventricular cells from hypertrophied rat hearts. *J Mol Cell Cardiol* **31**, 1617–1625.

Matteson DR & Armstrong CM (1986). Properties of two types of calcium channels in clonal pituitary cells. *J Gen Physiol* **87**, 161–182.

Murray KT, Fahrig SA, Deal KK, Po SS, Hu NN, Snyders DJ, Tamkun MM & Bennett PB (1994). Modulation of an inactivating human cardiac K^+ channel by protein kinase C. *Circ Res* **75**, 999–1005.

Murray KT, Hu NN, Daw JR, Shin HG, Watson MT, Mashburn AB & George AL Jr (1997). Functional effects of protein kinase C activation on the human cardiac Na^+ channel. *Circ Res* **80**, 370–376.

Newton AC (1995). Protein kinase C: structure, function, and regulation. *J Biol Chem* **270**, 28495–28498.

O'Dell TJ & Alger BE (1991). Single calcium channels in rat and guinea-pig hippocampal neurons. *J Physiol* **436**, 739–767.

Park JY, Jeong SW, Perez-Reyes E & Lee JH (2003). Modulation of $Ca_v3.2$ T-type Ca^{2+} channels by protein kinase C. *FEBS Lett* **547**, 37–42.

Pemberton KE, Hill-Eubanks LJ & Jones SV (2000). Modulation of low-threshold T-type calcium channels by the five muscarinic receptor subtypes in NIH 3T3 cells. *Pflugers Arch* **440**, 452–461.

Peretz T, Levin G, Moran O, Thornhill WB, Chikvashvili D & Lotan I (1996). Modulation by protein kinase C activation of rat brain delayed-rectifier K^+ channel expressed in *Xenopus* oocytes. *FEBS Lett* **381**, 71–76.

Perez-Reyes E (2003). Molecular physiology of low-voltage-activated T-type calcium channels. *Physiol Rev* **83**, 117–161.

Perez-Reyes E, Cribbs LL, Daud A, Lacerda AE, Barclay J, Williamson MP, Fox M, Rees M & Lee JH (1998). Molecular characterization of a neuronal low-voltage-activated T-type calcium channel. *Nature* **391**, 896–900.

Poole AW, Pula G, Hers I, Crosby D & Jones ML (2004). PKC-interacting proteins: from function to pharmacology. *Trends Pharmacol Sci* **25**, 528–535.

Schroeder JE, Fischbach PS & McCleskey EW (1990). T-type calcium channels: heterogeneous expression in rat sensory neurons and selective modulation by phorbol esters. *J Neurosci* **10**, 947–951.

Sheng ZH, Rettig J, Takahashi M & Catterall WA (1994). Identification of a syntaxin-binding site on N-type calcium channels. *Neuron* **13**, 1303–1313.

Singer-Lahat D, Gershon E, Lotan I, Hullin R, Biel M, Flockerzi V, Hofmann F & Dascal N (1992). Modulation of cardiac Ca^{2+} channels in *Xenopus* oocytes by protein kinase C. *FEBS Lett* **306**, 113–118.

Son WY, Lee JH, Lee JH & Han CT (2000). Acrosome reaction of human spermatozoa is mainly mediated by α_{1H} T-type calcium channels. *Mol Hum Reprod* **6**, 893–897.

Stea A, Soong TW & Snutch TP (1995). Determinants of PKC-dependent modulation of a family of neuronal calcium channels. *Neuron* **15**, 929–940.

Sun H, Hu XQ, Moradel EM, Weight FF & Zhang L (2003). Modulation of 5-HT_3 receptor-mediated response and trafficking by activation of protein kinase C. *J Biol Chem* **278**, 34150–34157.

Talavera K, Staes M, Janssens A, Droogmans G & Nilius B (2004). Mechanism of arachidonic acid modulation of the T-type Ca^{2+} channel α_{1G}. *J Gen Physiol* **124**, 225–238.

Tanabe T, Beam KG, Adams BA, Niidome T & Numa S (1990). Regions of the skeletal muscle dihydropyridine receptor critical for excitation-contraction coupling. *Nature* **346**, 567–569.

Toullec D, Pianetti P, Coste H, Bellevergue P, Grand-Perret T, Ajakane M, Baudet V, Boissin P, Boursier E, Loriolle F, Duhamel L, Charon D & Kirilovsky J (1991). The bisindolylmaleimide GF 109203X is a potent and selective inhibitor of protein kinase C. *J Biol Chem* **266**, 15771–15781.

Tsakiridou E, Bertollini L, de Curtis M, Avanzini G & Pape HC (1995). Selective increase in T-type calcium conductance of reticular thalamic neurons in a rat model of absence epilepsy. *J Neurosci* **15**, 3110–3117.

Tseng GN & Boyden PA (1991). Different effects of intracellular Ca^{2+} and protein kinase C on cardiac T and L Ca^{2+} currents. *Am J Physiol Heart Circ Physiol* **261**, H364–H379.

Vasilets LA, Schmalzing G, Madefessel K, Haase W & Schwarz W (1990). Activation of protein kinase C by phorbol ester induces downregulation of the Na^+/K^+-ATPase in oocytes of *Xenopus laevis*. *J Membr Biol* **118**, 131–142.

Welsby PJ, Wang H, Wolfe JT, Colbran RJ, Johnson ML & Barrett PQ (2003). A mechanism for the direct regulation of T-type calcium channels by Ca^{2+}/calmodulin-dependent kinase II. *J Neurosci* **23**, 10116–10121.

Wolfe JT, Wang H, Howard J, Garrison JC & Barrett PQ (2003). T-type calcium channel regulation by specific G-protein $\beta\gamma$ subunits. *Nature* **424**, 209–213.

Wolfe JT, Wang H, Perez-Reyes E & Barrett PQ (2002). Stimulation of recombinant $Ca_v3.2$, T-type, Ca^{2+} channel currents by CaMKIIγ_c. *J Physiol* **538**, 343–355.

Xiao GQ, Mochly-Rosen D & Boutjdir M (2003). PKC isozyme selective regulation of cloned human cardiac delayed slow rectifier K current. *Biochem Biophys Res Commun* **306**, 1019–1025.

Xiao GQ, Qu Y, Sun ZQ, Mochly-Rosen D & Boutjdir M (2001). Evidence for functional role of εPKC isozyme in the regulation of cardiac Na^+ channels. *Am J Physiol Cell Physiol* **281**, C1477–C1486.

Xiong Z, Sperelakis N, Noffsinger A & Fenoglio-Preiser C (1995). Ca^{2+} currents in human colonic smooth muscle cells. *Am J Physiol Gastrointest Liver Physiol* **269**, G378–G385.

Yamazaki J, Britton F, Collier ML, Horowitz B & Hume JR (1999). Regulation of recombinant cardiac cystic fibrosis transmembrane conductance regulator chloride channels by protein kinase C. *Biophys J* **76**, 1972–1987.

Yunker AM & McEnery MW (2003). Low-voltage-activated ('T-Type') calcium channels in review. *J Bioenerg Biomembr* **35**, 533–575.

Zhang Y, Cribbs LL & Satin J (2000). Arachidonic acid modulation of α_{1H}, a cloned human T-type calcium channel. *Am J Physiol Heart Circ Physiol* **278**, H184–H193.

Zheng X, Zhang L, Wang AP, Bennett MV & Zukin RS (1999). Protein kinase C potentiation of N-methyl-D-aspartate receptor activity is not mediated by phosphorylation of N-methyl-D-aspartate receptor subunits. *Proc Natl Acad Sci U S A* **96**, 15262–15267.

Zhou Z & Lipsius SL (1994). T-type calcium current in latent pacemaker cells isolated from cat right atrium. *Mol Cell Cardiol* **26**, 1211–1219.

Zhuang H, Bhattacharjee A, Hu F, Zhang M, Goswami T, Wang L, Wu S, Berggren PO & Li M (2000). Cloning of a T-type Ca^{2+} channel isoform in insulin-secreting cells. *Diabetes* **49**, 59–64.

Acknowledgements

This work was supported by the Korea Research Foundation Grant funded by the Korean Government (KRF-2005-015-C00403) to J.-H. Lee.